FEBS Letters 580 (2006) 3329–3334

Role of the leader sequence in tobacco pectin methylesterase secretion

Yuri L. Dorokhov[a], Eugene V. Skurat[a], Olga Yu. Frolova[a], Tatjana V. Gasanova[a], Peter A. Ivanov[a], Nikolay V. Ravin[b], Konstantin G. Skryabin[b], Kristiina M. Mäkinen[c], Viktor I. Klimyuk[d], Yuri Yu. Gleba[d], Joseph G. Atabekov[a,*]

[a] *Department of Virology, A.N. Belozersky Institute of Physico-Chemical Biology, Moscow State University, Leninsky Gory 1, Laboratory Building A, Moscow 119992, Russia*
[b] *Center "Bioengineering" Russian Academy of Science, Moscow 119992, Russia*
[c] *Department of Applied Biology, P.O. Box 27, University of Helsinki, 00014, Finland*
[d] *Icon Genetics GmbH, Biozentrum Halle, Weinbergweg 22, Halle, Germany*

Received 9 April 2006; revised 26 April 2006; accepted 28 April 2006

Available online 8 May 2006

Edited by Ulf-Ingo Flügge

Abstract **We report that unprocessed tobacco pectin methylesterase (PME) contains N-terminal pro-sequence including the transmembrane (TM) domain and spacer segment preceding the mature PME. The mature portion of PME was replaced by green fluorescent protein (GFP) gene and various deletion mutants of pro-sequence fused to GFP were cloned into binary vectors and agroinjected in *Nicotiana benthamiana* leaves. The PME pro-sequence delivered GFP to the cell wall (CW). We showed that a transient binding of PME TM domain to endoplasmic reticulum membranes occurs upon its transport to CW. The CW targeting was abolished by various deletions in the TM domain, i.e., anchor domain was essential for secretion of GFP to CW. By contrast, even entire deletion of the spacer segment had no influence on GFP targeting.**

Keywords: Pectin methylesterase; Transmembrane domain; Cell wall

1. Introduction

In the secretory pathway, transport of plant proteins occurs from the endoplasmic reticulum (ER) through the Golgi complex to the cell wall (CW) or vacuoles. The targeting of plant secretory proteins to the ER is an entry point for proteins destined for ER and different organelles [1]. The entry of proteins into the endomembrane system depends on the presence of a transient N-terminal pro-sequence (PS) that is characterized by a stretch of mainly apolar residues [2]. In addition to their function in targeting, pro-sequences play an important role in protein topogenesis by orienting themselves in the translocon and membrane. Four classes of single-spanning membrane proteins can be distinguished according to their orientation in the bilayer and on the topogenic sequences that direct their insertion into the ER membrane [3].

The CW-associated pectin methylesterase (PME) is a ubiquitous plant enzyme that catalyzes the pectin deesterification by forming carboxylates and methanol. In higher plants the PME genes encode N-terminal leader PS of different length required for protein targeting to ER; the leader includes the transmembrane (TM) domain and spacer sequence (SS). It was hypothesized that SS plays the role in a subcellular targeting acting as an intramolecular chaperone in folding of mature enzyme, or as autoinhibitor during transport through the endomembrane system [4,5].

Here, we isolated and sequenced the full-size tobacco full-length PME gene including the 5′-sequence coding for the N-terminal PME pro-sequence region (proPME) cDNA. Intracellular PME targeting was studied in transient expression experiments by agroinjection of *Nicotiana benthamiana* leaves. Our results showed that the TM, but not the SS domain of PME PS was indispensable for TM-green fluorescent protein (GFP) delivery into apoplastic space and CW. The evidence was provided that expression of TM-GFP leads to transient binding of the PME TM domain to ER membranes, i.e., PME uses the membrane anchoring feature to mediate its transport to the cell surface.

2. Materials and methods

2.1. Isolation of full-length PME gene from N. tabacum

A tobacco (*N. tabacum*) cDNA library comprised of 1.5×10^6 independent clones in lambda NM1149 vector was kindly provided by Dr. W. Rohde. Plaques (10^5 per 400 cm^2 plate) were screened as described [6] using hybridization probe [7]. The clone termed proPME-1 (EMBL Accession No. AJ401158) was cloned into the plant expression vector pBIN19 [8] and designated as pBIN-proPME.

2.2. Expression plasmids

pBIN-proPME gene in antisense orientation (as-proPME), carrying the proPME in the reverse orientation with respect to the 35S promoter, was used to express RNA, complementary to the plus strand of the PME gene.

The active site of the PME enzyme from carrot was described using crystal structure analysis [9,10]. To obtain enzymatically inactive PME, two conservative amino acids in the active site of the enzyme were substituted by overlapping PCR using primers QD(+)

*Corresponding author. Fax: +7 495 938 0601.
E-mail address: atabekov@genebee.msu.su (J.G. Atabekov).

Abbreviations: aa; amino acid; proPME, full-length PME gene including the 5′-sequence coding for the N-terminal PME pro-sequence region; as-proPME, proPME gene in antisense orientation; BFA, brefeldin A; CW, cell wall; ER, endoplasmic reticulum; GFP, green fluorescent protein; MP, movement protein; PME, mature, processed pectin methylesterase; PME(395A396A), PME mutant with Ala substitutions in its active center; PS, N-terminal pro-sequence; SS, spacer sequence; TM, transmembrane

0014-5793/$32.00
doi:10.1016/j.febslet.2006.04.090

CATTTTAGCCTATGCAGCCTCTCTCTACG and QD(−) GTAGAGAGAGGCTGCATAGGCTAAAATG. The resulting sequence carried mutations $Q_{395} \rightarrow A$ and $D_{396} \rightarrow A$. The mutant gene was sequenced and cloned into pBIN19 together with the 35S promoter and nopalin synthase gene (nos) terminator sequences. The final construct pBIN-proPME(395A396A), was transformed into *Agrobacterium tumefaciens* strain GV 3101.

2.3. Deletions in the PS region of proPME

Two series of PME deletion variants were obtained using overlap PCR. A-series of deletions made in a putative PME TM anchor region included: A1 (17–23 aa), A2 (17–29 aa) and A3 (complete deletion of TM). B-series of PME deletions made in the SS of PS downstream of TM region included: B1 (40–125 aa), B2 (40–148 aa), B3 (190–248 aa) and B4 (deletion of the whole SS). PS region and its deletion variants were cloned using *Nco*I and *Bam*HI sites into GFP expressing vector based on pCAMBIA1300 in order to obtain PS-GFP fusions under the control of 35S promoter. *A. tumefaciens* strain GV3101 was transformed by these plasmids and used in agroinjection experiments together with another *Agrobacterium* carrying HcPro gene (the protein-suppressor of gene silencing taken from potato virus Y genome).

2.4. Agroinjection procedure

Agrobacterium tumefaciens strain GV3101 was grown at 28 °C in LB media supplemented with 50 μg ml^{-1} rifampicin and 25 μg ml^{-1} gentamicin to the stationary phase. Bacterial cultures were centrifuged at $5000 \times g$ for 5 min at room temperature and resuspended in 10 mM $MgSO_4$ MES, pH 5.6. Cells were incubated in this medium for 3 h and then infiltrated into the abaxial air spaces of 4-week-old *N. benthamiana* plants. Injection of bacterial cultures containing the constructs described above was performed with suspensions at $OD_{600} = 0.6$.

2.5. Isolation of CW and apoplastic proteins

Isolation of CW fraction and CW-associated proteins was carried out as described [7]. The apoplastic proteins were isolated by vacuum infiltration as described [11].

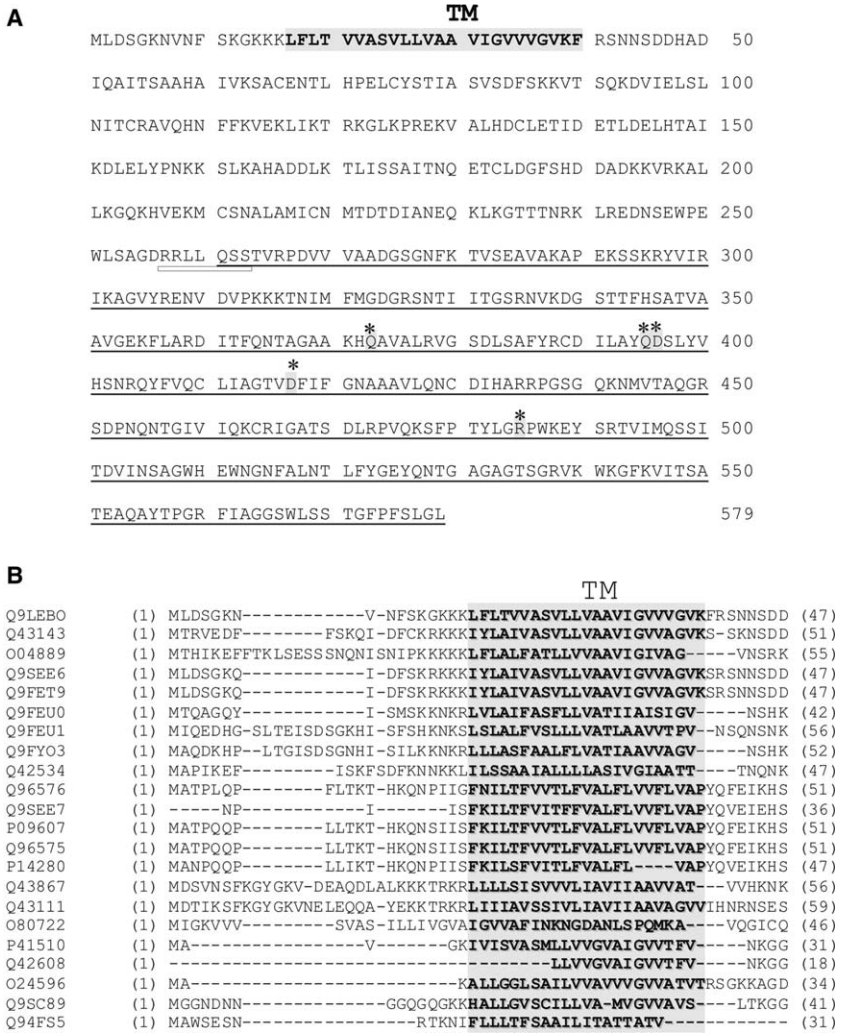

Fig. 1. Amino acid sequence of unprocessed tobacco PME. (A) Amino acid sequence of tobacco (Q9LEBO) PME. Putative mature PME is underlined. Asterisks indicate the conserved residues constituting a proposed active site of PME. The PME PS TM domain identified by the SOSUI program (http://sosui.proteome.bio.tuat.ac.jp) is highlighted. Empty bar indicates putative processing site. (B) Amino acid sequence alignment of N-terminal part of 22 selected PME PS performed with the GeneBee program (http://www.belozersky.msu.ru). Data were taken from SWISSPROT databank and website (http://afmb.cnrs-mrs.fr/CAZY/CE_8.html). Selected PMEs belong to different clades based on evolutionary tree [4]. Clade 1: Accession No. Q9LEBO for *N. tabacum*, Q43143 for *Lycopersicon esculentum*, O04889 for *Camellia sinensis*, Q9SEE6 for *Solanum tuberosum*, Q9FET9 (pme4), Q9FEUO (pme3) and Q9FEU1 (pme2), Q9FY03 (pmel) for *P. tremula*, Q42534 for *Arabidopsis thaliana*. Clade 2: Q96576 for *L. esculentum*, Q9SEE7 for *S. tuberosum*, P09607, P96575 and P14280 for *L. esculentum*. Clade 3: Q43867 for *A. thaliana*, Q43111 for *Phaseolus vulgaris*. Clade 4: O80722 for *A. thaliana*, P41510 for *Brassica napus*, Q42608 for *Brassica rapa*, O24596 for *Zea mays*, Q9SC89 for *Medicago truncatula*; Q94FS5 for unclassified *L. usitatissimum* (flax) PME. Numerals in brackets designate the amino acid position.

2.6. Western blot analysis

Total proteins isolated from leaves were subjected to SDS–polyacrylamide gel electrophoresis and blotted onto polyvinylidene difluoride membranes (Amersham, Arlington Heights, III). The membranes were probed with affinity-purified rabbit antibodies that were raised against GFP or mature PME. Goat anti-rabbit IgG conjugated with horseradish peroxidase (Sigma) were used as the secondary antibody and the reaction was visualized by chemiluminescence (ECL System, Amersham Pharmacia).

2.7. PME enzymatic assay

PME activity of plant leaf tissue was quantified by a gel diffusion assay [12,13].

2.8. GFP imaging

The GFP fluorescence was monitored by epi-illumination with a handheld UV source (DESAGA). A dissecting microscope (Opton IIIRS), coupled to an epifluorescence module, was used for single cell observations. Lower epidermal cells of transformed leaves were analyzed at 72 h after agroinjection. Confocal imaging was performed using an inverted Zeiss LSM 510 laser scanning microscope (Jena, Germany).

3. Results

3.1. Isolation of the full-size PME gene of N. tabacum *and its expression in* N. benthamiana *(agroinjection experiments)*

Previously, the 3′-terminal part of PME mRNA containing the region coding for mature PME has been amplified by RT-PCR, isolated, cloned and sequenced [7]. Here we isolated the full-length proPME gene from a tobacco cDNA library. The deduced amino acid (aa) sequence (Fig. 1A) of one of the full-length tobacco cDNA clones (EMBL Accession No. AJ401158; SWISSPROT Databank Accession No. Q9LEBO) belongs to PME clade Plant 1 [4]. Unprocessed proPME protein contained the 255-aa long N-terminal leader (PS) preceding the 319-aa mature PME portion (Fig. 1A, underlined sequence). The PME from *Daucus carota* (P83218) might be considered as the type member of this clade, since its 3D structure was reported [9]. The sequences of mature PMEs of different origins are very similar and amino acid residues at the active site are highly conserved: two aspartic acids, arginine, two glutamines and most of aromatic residues lining the cleft [9,10] (Fig. 1A). The carrot PME N-terminal blocking group was found to start with pyroglutamate, derived from cyclization of an the N-terminal glutaminyl residue. This might explain the nature of the blocked N terminus [9,10]. It could be proposed that RRLL-QSS motif serves as the PME processing site.

A characteristic TM was revealed in the N-proximal region of tobacco PME (Fig. 1A). It represented the 24-aa segment enriched with hydrophobic amino acids preceded by a more positive flanking sequence. This domain could be revealed in several PMEs belonging to different clades (Fig. 1B). Presumably, the tobacco PME can be regarded as a type II membrane protein [14,15]. In addition, the PS PME sequence contains a long (aa 39–255) SS located between the TM and the mature portion of enzyme.

In a series of experiments, the contribution of *Agrobacterium*-mediated expression of full-length PME gene to the CW-associated enzymatic activity of *N. benthamiana* leaves

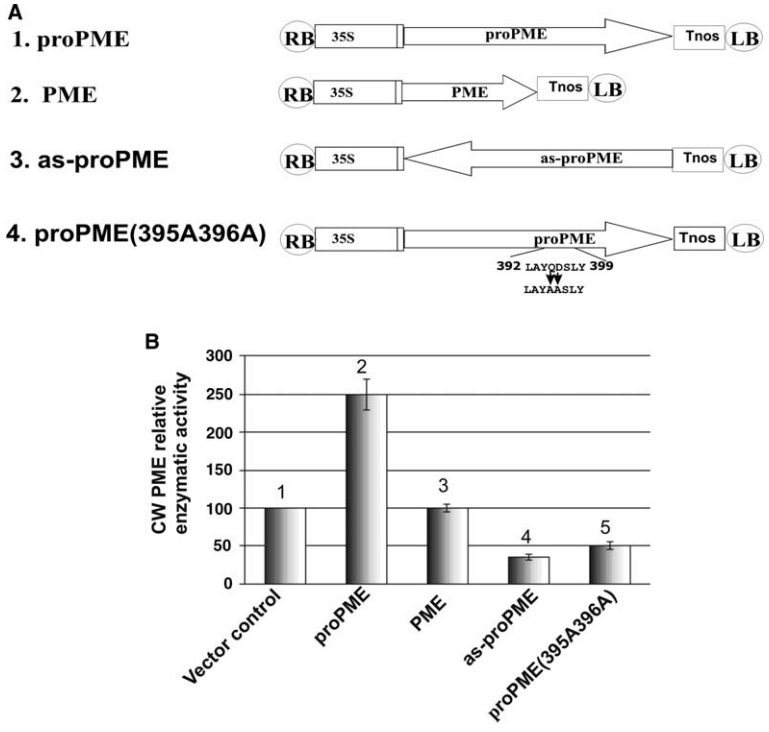

Fig. 2. Substitution mutations in a putative active center abolished the PME enzymatic activity. (A) Schematic representation of binary vectors containing the full-length proPME gene and its derivatives: (1) proPME, the full-length tobacco PME gene (EMBL Accession No. AJ401158); (2) PME, mature PME lacking PS; (3) as-proPME, tobacco PME gene in the antisense orientation; (4) proPME(395A396A), PME mutant with the amino acids (395Q and 396D) (see Fig. 1) substituted by alanines. All constructs were based on the T-DNA of the pBin19 binary vector. LB and KB indicate the left and right borders of T-DNA, respectively. Tnos, transcription terminator of nopaline synthase gene (NOS). (B) PME enzymatic activity in CW fractions from leaves agroinjected with PME cDNA and its derivatives. The CW-associated PME activity in leaves, agroinjected with empty vector was taken as 100 U. The mean values (with S.E. bars) for 3–5 independent experiments are given.

was examined using the binary vectors containing: (i) the wild-type tobacco proPME gene (Fig. 2A1), (ii) mature PME lacking PS (Fig. 2B3), (iii) as-proPME (Fig. 2A3) and (iv) proPME substitution mutant with Asn395 and Asp396 replaced by alanines in a putative active center of PME (Fig. 2A4). Fig. 2B2 shows that the CW-associated PME enzymatic activity increased significantly after agroinjection with proPME gene. Apparently, increase of PME synthesis was directed by plant, but not by agrobacterial cells; our control experiments confirmed that bacterial culture medium and bacterial extracts exhibited no PME activity. In addition, the level of CW-associated PME activity was not affected by expression of mature PME lacking PS (Fig. 2B3). Thus, the PS was essential for PME targeting to CW. Enzymatic activity of CW-associated PME was significantly reduced in leaves agroinjected with as-proPME construct (Fig. 2B4). This result was in line with the data obtained with tomato leaves [16] and fruits [17]. Furthermore, expression of the PME mutant with Ala substitutions in its active center (PME(395A396A)) mutant gene encoding inactive enzyme strongly inhibited CW-associated PME activity (Fig. 2B5), whereas, the total amount of PME protein revealed by Western analyses in CW fraction increased markedly (data not shown). The effect of PME(395A396A) mutant expression could be due to the competition between endogenous PME and exogenous PME mutant protein, and/or to the capacity of proPME(395A396A) to suppress PME-mediated gene silencing.

3.2. TM anchor domain of PME PS, but not the SS is required for GFP delivery to CW

The PME TM as a single topogenic domain was likely to function both as signal and anchor for insertion into ER membrane. To visualize process of secretion, the PS-GFP construct was used, where PME PS was fused to a foreign GFP gene (Fig. 3A). After agroinjection of PS-GFP (Fig. 3B) GFP was targeted to the CW of epidermal cells. No accumulation of GFP in nuclei and cytoplasm was observed. The same picture was observed in epidermal cells of transgenic tobacco stably transformed with proPME:GFP taken as a control (data not shown). Therefore, the construct containing intact PME PS region fused to the GFP gene provided the means for the delivery of GFP to CW.

In order to demonstrate that transient binding of the PME TM domain to ER membranes mediates its transport to the cell surface, we used brefeldin A (BFA) to block the secretory trafficking pathway. BFA is known to cause redistribution of proteins from Golgi to the ER in tobacco leaf epidermal cells [19–23]. A strong ER labeling was observed when the PS-GFP-expressing leaf tissues were incubated with BFA (Fig. 3C). These results suggested that the PME TM domain in PS-GFP performed its membrane anchoring features during transport to the cell surface.

Various deletion mutants of PME PS (described in Section 2.3) were constructed to elucidate the role in PME intracellular trafficking and secretion of (i) a hydrophobic TM (A-series

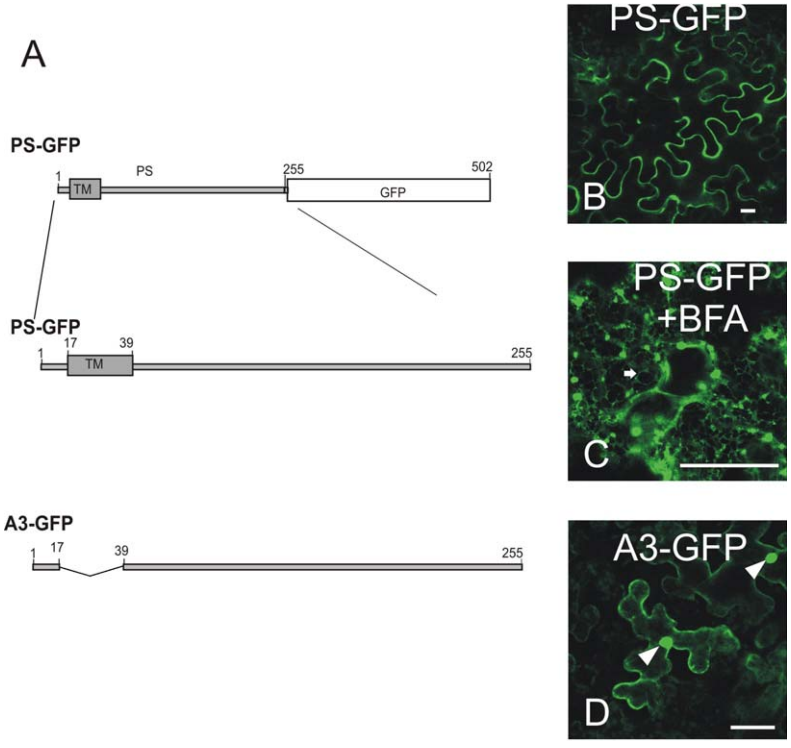

Fig. 3. The TM domain of PME PS is required for delivery of a chimeric PS-GFP to CW. (A) PS-GFP construct–PME PS sequence was fused to that of GFP gene instead of mature PME and used for obtaining A3-GFP mutant lacking TM. Arabic numerals designate amino acid positions. (B–D) Confocal microscopy of epidermal cells of *N. benthamiana* leaves 2–3 days after agroinjection with PS-GFP construct and A3-GFP mutant lacking TM. (B) The PME leader sequence provides intracellular trafficking of GFP to CW. (C) Effect of BFA on PS-GFP distribution. BFA (100 μg/ml) was added to block secretory pathway and cells were observed 2 h later. Fluorescence of polygonal ER structure is marked by arrow. (D) Deletion of TM domain of PS abolished the CW targeting of GFP. Arrowhead indicates nuclei stained by GFP. Scale bars: 20 μm.

PS:GFP mutants) and (ii) the 216-aa long SS located between the TM and mature portion of enzyme (B-series PS:GFP mutants). The epidermal cells of *N. benthamiana* leaves were agroinjected with the mutant constructs and GFP was visualized by confocal laser scanning microscopy. The deletions in TM suppressed significantly the CW targeting ability of GFP. Fig. 3D shows that the CW targeting of GFP by A3-GFP mutant lacking the entire TM domain was reduced, resulting in a characteristic cytoplasmic and nuclear GFP staining [24]. Contrary to TM-mutants, the B-series mutants, displayed the CW targeting of GFP indistinguishable from that produced by proPME:GFP; even entire deletion of the spacer segment had no influence on GFP targeting (data not shown).

Our results implied that GFP accumulates in apoplastic space of leaves transiently expressing either proPME:GFP or PS-GFP constructs. The apoplastic proteins were isolated from agroinjected leaves by vacuum-infiltration and subsequent extraction. Total proteins of apoplastic liquor and the proteins of the remnant leaf material were examined by Western blotting with anti-GFP antibodies. Analysis of remnant material from leaves transiently expressing PS-GFP revealed (besides a minor band of approximately 40 kDa) two major protein bands apparently corresponding to mature GFP (27 kDa) and partly processed 60 kDa PS-GFP (33 + 27 kDa), respectively (Fig. 4A). Likewise, the remnant material from leaves agroinjected by PS mutants of A-series contained a major GFP and 60-kDa bands. It is noteworthy that the B4-GFP construct lacking a SS between the TM PME domain and the GFP produced a major protein band of expected size (Fig. 4A).

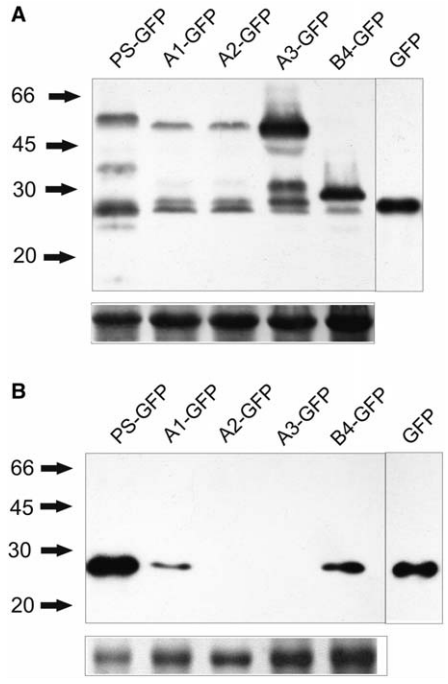

Fig. 4. Deletions in TM of PS-GFP abolish the secretion of GFP into the apoplastic space. *N. benthamiana* leaves were examined 2–3 days after agroinjection with PS-GFP and its deletion variants. For detailed description of the mutants, see Section 2.3. Plant material was vacuum infiltrated and proteins of apoplastic extract and remnant leaves were probed with anti-GFP antibodies. (A, B) Western analysis of the remnant leaf material (A) and apoplastic proteins (B). Bacterially expressed GFP was used as a positive control (GFP slot). The equal loading of leaf proteins was confirmed by appearance of large subunit of RUBISCO (RbsL) (A) and unknown apoplastic protein (B).

Examination of apoplastic proteins of PS-GFP samples revealed only the mature GFP (Fig. 4B). Small amount of GFP could be observed in apoplastic space of leaves agroinjected with A1-GFP mutant, however, no GFP could be found in apoplastic protein fractions from leaves agroinjected with A2-GFP and A3-GFP deletion mutants. By contrast, B4-GFP mutant retained secretory capacity and GFP could be revealed by Western blot analysis. These data taken together with our confocal microscopy studies, indicated that TM is indispensable, whereas the SS was not required for GFP delivery into apoplastic space and CW.

4. Discussion

PME is involved in CW growth and development, root development [25], stem elongation, pollen tube growth and fruit ripening [26]. Previously, we showed that tobacco PME was able to interact with TMV movement protein (MP) [7]. It is believed that the CW-associated PME of *N. tabacum* acts as a host-receptor for TMV MP and this interaction is required for TMV movement [7,27,28].

The PME sequences were recently aligned and evolutionary tree was calculated [4] where plant enzymes were grouped into eight separate clades. Tobacco PME (Fig. 1A) belongs to clade Plant 1 with long (255-aa) leader sequence and five conserved regions characteristic for mature PME.

To study the PME processing and CW targeting, unprocessed PME and its derivatives were transiently expressed in *N. benthamiana* cells by agroinjection (Fig. 2). The CW-associated PME enzymatic activity was significantly stimulated by wild-type PME gene expression and drastically suppressed after expression of antisense PME construct.

Crystal structure of carrot mature PME showed that the highly conserved residues at the active site are the two aspartic acids (Asp136 and Asp137), the arginine (Arg225), two glutamines (Gln113 and Gln135) and most of the aromatic residues lining the shallow cleft [9,10]. We constructed the enzymatically inactive PME mutant (395A396A) with Gln395 (corresponding to carrot Gln135) and Asp396 (corresponding to carrot Asp136) substituted by alanines.

Analysis of the tobacco PME sequences revealed a signal sequence and TM domain containing the 24-aa stretch enriched with hydrophobic amino acids; this domain found in PME of different clades was preceded by a more positive N-terminal flanking sequence characteristic of type II membrane proteins [14,15].

To visualize process of secretion, the chimeric fusion constructs were made, where the PME PS was fused to that of foreign GFP gene (PS-GFP). Transient expression of these constructs provided the means for the delivery of GFP to CW. The crucial role of the TM domain in tobacco PME secretion was confirmed: it has been shown by deletion analysis that the TM anchor domain, but not the 216-aa SS between TM and mature portion of PME was required for GFP delivery to CW. To demonstrate that transient binding of the PME TM domain to ER membranes mediates its transport to the cell surface, BFA was used to block the secretory traffic. PS:GFP trafficking in CW was inhibited and fluorescence of

polygonal ER structure was observed (marked by arrow in Fig. 3C). Remarkably, the B4-GFP mutant protein used in these experiments represented the N-proximal PME TM domain fused directly to GFP gene. These results suggested that ER-membrane anchoring features of PME TM are involved in its transport to the cell surface.

Acknowledgements: The authors thank Professor Dr. W. Rohde (Max-Planck-Institut fuer Zuchthungsforshung, Cologne) for generously providing the cDNA library in lambda NM1149 vector. This work was partly supported by the Russian Academy of Science (Programme "Molecular and Cellular Biology"), Russian Foundation for Basic Research (Grants 04-04-48490, 05-04-48674 and 05-04-08002) and Russian Federal Agency of Science and Innovations (Contract 02.435.11.3012).

References

[1] Vitale, A. and Denecke, J. (1999) The endoplasmic reticulum – gateway of the secretory pathway. Plant Cell 11, 615–628.
[2] Walter, P. and Johnson, A.E. (1994) Signal sequence recognition and protein targeting to the endoplasmic reticulum membrane. Annu. Rev. Cell. Biol. 10, 87–119.
[3] Spiess, M. (1995) Heads or tails – what determines the orientation of proteins in the membrane. FEBS Lett. 369, 76–79.
[4] Markovič, O. and Janeček, Š. (2004) Pectin methylesterases: sequence-structural features and phylogenetic relationships. Carbohydrate Res. 339, 2281–2295.
[5] Micheli, F. (2001) Pectin methylesterases: cell wall enzymes with important roles in plant physiology. Trends Plant Sci. 6, 414–419.
[6] Sambrook, J., Fritsch, E.F. and Maniatis, T. (1989) Molecular Cloning: A Laboratory Manual, 2nd edn, Cold Spring Harbor Laboratory Press, Cold Spring Harbor, NY.
[7] Dorokhov, Y.L., Makinen, K.M., Frolova, O.Yu., Merits, A., Kalkkinen, N., Saarinen, J., Atabekov, J.G. and Saarma, M. (1999) A novel function for a ubiquitous plant enzyme pectin methylesterase: the host-cell receptor for the tobacco mosaic virus movement protein. FEBS Lett. 461, 223–228.
[8] Bevan, M. (1984) Binary *Agrobacterium* vectors for plant transformation. Nucleic Acids Res. 12, 8711–8721.
[9] Johansson, K., El-Ahmad, M., Friemann, R., Jörnvall, H., Markovič, O. and Eklund, H. (2002) Crystal structure of plant pectin methylesterase. FEBS Lett. 514, 243–249.
[10] Marcovič, O., Cederlund, E., Griffiths, W.J., Lipka, T. and Jörnvall, H. (2002) Characterization of carrot pectin methylesterase. Cell Mol. Life Sci. 59, 513–518.
[11] Hon, W.-C., Griffith, M., Chong, P. and Yang, D.S.C. (1994) Extraction and isolation of antifreeze proteins from winter rye (*Secale cereale* L.) leaves. Plant Physiol. 104, 971–980.
[12] Downie, B., Dirk, L.M.A., Handfield, K.A., Wilkins, T.A., Bennett, A.B.B. and Bradford, K.J. (1998) A gel diffusion assay for quantification of pectin methylesterase activity. Anal. Biochem. 264, 149–157.
[13] Chen, M.-H. and Citovsky, V. (2003) Systemic movement of a tobamovirus requires host cell pectin methylesterase. Plant J. 35, 386–392.
[14] Goder, V. and Spiess, M. (2003) Molecular mechanism of signal sequence orientation in the endoplasmic reticulum. EMBO J. 22, 3645–3653.
[15] Hartmann, E., Rapoport, T.A. and Lodish, H.F. (1989) Predicting the orientation of eukaryotic membrane-spanning proteins. Proc. Natl. Acad. Sci. USA 86, 5786–5790.
[16] Gaffe, J., Tiznado, M.E. and Handa, A.K. (1997) Pectin methylesterase isoforms in tomato (*Lycopersicon esculentum*) tissues. Effects of expression of a pectin methylesterase antisense gene. Plant Physiol. 114, 1547–1556.
[17] Tieman, D.M., Harriman, R.W., Ramomahan, G. and Handa, A.K. (1992) An antisense pectin methylesterase gene alters pectin chemistry and soluble solids in tomato fruit. Plant Cell 4, 667–679.
[19] Boevink, P., Oparka, K., Santa-Cruz, S., Martin, B., Betteridge, A. and Hawes, C. (1998) Stacks on tracks: the plant Golgi apparatus traffics on an actin/ER network. Plant J. 15, 441–447.
[20] Brandizzi, F., Snapp, E.L., Roberts, A.G., Lippincott-Schwartz, J. and Hawes, C. (2002) Membrane protein transport between the endoplasmic reticulum and the Golgi in tobacco leaves is energy dependent but cytoskeleton independent: evidence from selective photobleaching. Plant Cell 14, 1293–1309.
[21] Chatre, L., Brandizzi, F., Hocquellet, A., Hawes, C. and Moreau, P. (2005) Sec22 and Memb11 are v-SNAREs of the anterograde endoplasmic reticulum-Golgi pathway in tobacco leaf epidermal cells1. Plant Phys. 139, 1244–1254.
[22] daSilva, L.L.P., Snapp, E.L., Denecke, J., Lippincott-Schwartz, J., Hawes, C. and Brandizzi, F. (2004) ER export sites and Golgi bodies behave as single mobile secretory units in plant cells. Plant Cell 16, 1753–1771.
[23] Saint-Jore, C.M., Evins, J., Batoko, H., Brandizzi, F., Moore, I. and Hawes, C. (2002) Redistribution of membrane proteins between the Golgi apparatus and endoplasmic reticulum in plants is reversible and not dependent on cytoskeletal networks. Plant J. 29, 661–678.
[24] Brandizzi, F., Hanton, S., daSilva, L.L.P., Boevink, P., Evans, D., Oparka, K., Denecke, J. and Hawes, C. (2003) ER quality control can lead to retrograde transport from the ER lumen to the cytosol and the nucleoplasm in plants. Plant J. 34, 269–281.
[25] Wen, F.S., Zhu, Y.M. and Haves, M.C. (1999) Effect of pectin methylesterase gene expression on pea root development. Plant Cell 11, 1129–1140.
[26] Bosch, M. and Hepler, P.K. (2005) Pectin methylesterases and pectin dynamics in pollen tubes. Plant Cell 17, 3219–3226.
[27] Chen, M.-H., Sheng, J., Hind, G., Handa, A.K. and Citovsky, V. (2000) Interaction between the tobacco mosaic virus movement protein and host cell pectin methylesterases is required for viral cell-to-cell movement. EMBO J. 19, 913–920.
[28] Waigmann, E., Ueki, S., Trutneva, K. and Citovsky, V. (2004) The ins and outs of nondestructive cell-to-cell and systemic movement of plant viruses. Crit. Rev. Plant Sci. 23, 195–250.